

Influence of Surface Protonation–Deprotonation Stimuli on the Chiroptical Responses of (*R*)-/(*S*)-Mercaptosuccinic Acid-protected Gold Nanoclusters

Ryota Ueno and Hiroshi Yao*

Graduate School of Material Science, University of Hyogo, 3-2-1 Koto, Kamigori-cho, Ako-gun, Hyogo 678-1297

(E-mail: yao@sci.u-hyogo.ac.jp)

Racemic mixtures of mercaptosuccinic acid (MSA) are optically resolved to obtain enantiopure (*R*)-/(*S*)-MSA, and the (*R*)-/(*S*)-MSA-protected gold nanoclusters are synthesized. Circular dichroism responses of the nanoclusters are strongly dependent on the pH of the solution. In particular, chiroptical enhancement is observed under highly acidic conditions, which can be due both to the electronic and conformational origins of the surface chiral MSA ligand.

Gold nanoclusters with the diameter reduced to the order of the metal's Fermi wavelength are the most extensively studied due to their relative ease of preparation and interesting photophysical properties.¹ In particular, thiolate-protected gold nanoclusters are of importance and have attracted increasing interest both experimentally and theoretically. Mercaptosuccinic acid (MSA, IUPAC name: sulfanylsuccinic acid) is an intriguing thiol molecule to protect Au nanoclusters for biological applications because of its high water solubility and/or biocompatibility.² Indeed, the synthesis, characterization, and self-assembling processes of MSA-protected Au nanoclusters have been reported.³ On the other hand, MSA molecules on the bulk gold surface have been studied by surface-enhanced Raman spectroscopy (SERS),⁴ and it was found that MSA chemisorbs via both sulfur atom and one carboxy group (closer to the sulfur atom) dissociated at natural (or slightly acidic) pH.⁴ The influence of the solution pH on its monolayer structure has also been examined.⁴ Meanwhile, MSA is a chiral compound, although only the racemate is commercially available. If enantiopure MSA can be used to obtain optically active Au nanoclusters, the ligand protonation–deprotonation stimuli would control their chiroptical responses; thereby we can better understand the origin of the optical activity of the chiral thiolate-protected Au nanoclusters. In the present study, enantiopure (*R*)-/(*S*)-MSA is used to synthesize monolayer-protected Au nanoclusters. Racemic MSA is first optically resolved using a chiral amine molecule. Then the pH-responsive circular dichroism (CD) is examined. We believe this study will give an approach for finding strong optically active nanomaterials.

The optical resolution of racemic MSA (*rac*-MSA) was conducted using (*S*)-1-phenylethylamine (*S*-PEA) according to the literature.⁵ Briefly, *rac*-MSA and (*S*)-PEA were first dissolved in 1-propanol. After keeping the solution at -10°C overnight, the precipitate (*R*)-MSA·(*S*)-PEA was collected by filtration. The precipitate was recrystallized, yielding pure (*R*)-MSA·(*S*)-PEA. To obtain diastereomeric (*S*)-MSA·(*S*)-PEA, on the other hand, the filtrate was evaporated. Next, an aqueous solution containing (*R*)-MSA·(*S*)-PEA or (*S*)-MSA·(*S*)-PEA was treated with an Amberlite IR-120B ion-exchange resin in the H^+ form. Consequently, (*R*)-MSA or (*S*)-MSA was obtained after recrystallization (Figure 1a). The synthesis of (*R*)-/(*S*)-MSA-protected Au nanoclusters involves the preparation of an aqueous Au–thiolate

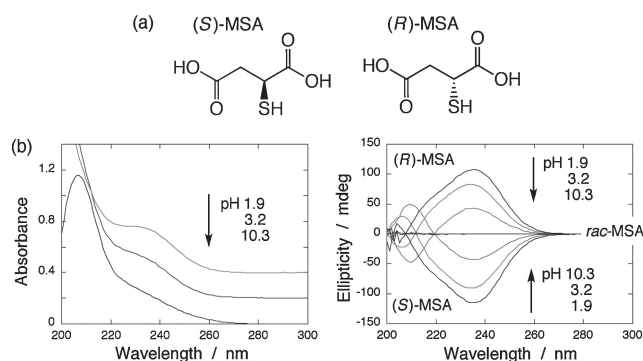


Figure 1. (a) Chemical structures of (*S*)-MSA and (*R*)-MSA. (b) (Left) Absorption spectra of (*R*)-MSA in aqueous solution at pH 1.9, 3.2, and 10.3. Spectra are offset by a constant for clarity. (Right) CD spectra of (*R*)-/(*S*)-/*rac*-MSA in aqueous solution at pH 1.9, 3.2, and 10.3.

complex followed by the reduction of the metal ions with NaBH_4 under a fixed MSA/Au molar ratio (= 2.0), which can be referred to as Au-(*R*)-MSA and Au-(*S*)-MSA, respectively.³ The precipitate was completely washed with water/methanol and ethanol repeatedly through a redispersion–centrifugation process to remove undesirable impurities. Finally, the precipitate dissolved in a small amount of water was freeze-dried.

MSA has three possibilities for acid dissociation, and the corresponding $\text{p}K_{\text{a}}$ values reported are; $\text{p}K_{\text{a}1} = 3.30$, $\text{p}K_{\text{a}2} = 4.94$, and $\text{p}K_{\text{a}3} = 10.64$, where $\text{p}K_{\text{a}1}$ ($\text{p}K_{\text{a}2}$) refers to the dissociation of a carboxy group that is closer (more distant) to the sulfur atom, and $\text{p}K_{\text{a}3}$ to thiol group deprotonation.⁴ UV absorption and the corresponding CD spectra of (*R*)-/(*S*)-MSA in aqueous solutions of pH 1.9, 3.2, and 10.3 are shown in Figure 1b. At pH 1.9, MSA has an absorption peak at ca. 235 nm, but the peak becomes blurred and weakened at higher pH values. The intensity of the Cotton effects at ca. 235 nm is also a function of pH (Figure 1b); the CD response is increased with a decrease in the pH value. Note that a red-tail absorption observed at ca. 260 nm at pH 10.3 is a property of sulfide anions.⁶ In general, thiol groups ($-\text{SH}$) have no absorption in the wavelength region longer than ca. 220 nm.⁶ In addition, we confirmed that succinic acid did not show any absorption at \geq ca. 220 nm under the highly acidic condition. Hence, to identify this peak of MSA, quantum chemical calculations were conducted. We chose three forms of MSA on the carboxy protonation–deprotonation; that is, neutral, singly, and doubly deprotonated species. The calculation required several steps: In the first step, a conformational optimization was conducted for the chosen stereoisomer to obtain a local minimal energy with the Gaussian 09 program at the density functional theory (DFT) level using the B3PW91 functional and a 6-31+G* basis set.⁷ Three typical, staggered conformations produced by

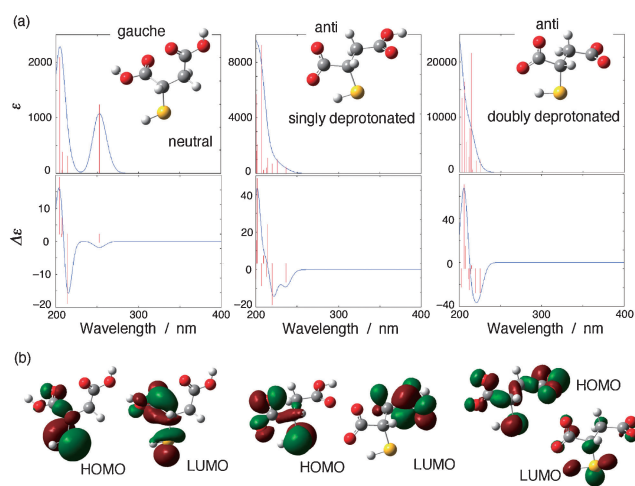


Figure 2. Optimized conformations of neutral (left), singly (middle), and doubly (right) deprotonated forms of (*S*)-MSA, along with the corresponding absorption and CD spectra simulated, respectively. (b) HOMO and LUMO images of various forms of (*S*)-MSA.

rotation around the C₂–C₃ axis were considered. Next, for the lowest-energy geometry, time-dependent DFT (TD-DFT) calculations were performed, obtaining the oscillator strength (ϵ) and rotatory strength ($\Delta\epsilon$). To include solvent (water) effects, the conductor polarizable continuum model (C-PCM) present in Gaussian 09 was used.⁷

Results on the optimized geometry as well as the corresponding absorption and CD spectra of neutral, singly or, doubly deprotonated (*S*)-MSA are shown in Figure 2a. The lowest-energy transition is dominated by the HOMO–LUMO transition (Figure 2b). In neutral MSA, the gauche conformation is stable, and from the orbital pictures of the HOMO and LUMO, we can determine that the absorption peak of ca. 235 nm observed at pH 1.9 is due principally to the $n\text{--}\pi^*$ transition of C=O coupled with the proximal sulfur atom. Upon deprotonation, both the electronic structure and stable conformation of MSA were significantly modulated; for example, the stable conformation of singly or doubly deprotonated MSA was an anti form, and the HOMO–LUMO transition, having a charge-transfer (CT) nature as judged from Figures 2b and 2c, shifted to a higher energy. The $n\text{--}\pi^*$ transitions of C=O were also shifted to more blue, in good agreement with the observed data (Figure 1b). Note that the calculations showed a difference from the experimental data on the disappearance of the spectroscopic response at ca. 235 nm. This may suggest that other conformers having different absorption and CD responses (= electronic natures) should also be present in high-pH solutions.⁸

Metal nanoclusters with chirality are attractive for their stereochemistry.⁹ Hence, to examine how the modulation of the electronic states of chiral MSA ligands upon protonation–deprotonation stimuli influences the chiroptical responses of the MSA-protected Au nanoclusters, we next evaluated Au–(*R*)-MSA and Au–(*S*)-MSA samples. We first determined the mean core size and typical size distribution of the Au–MSA samples by STEM observations (Figure 3a). Both samples had similar size and distribution, and according to the micrographs, we could determine the mean diameters of 1.5 nm.

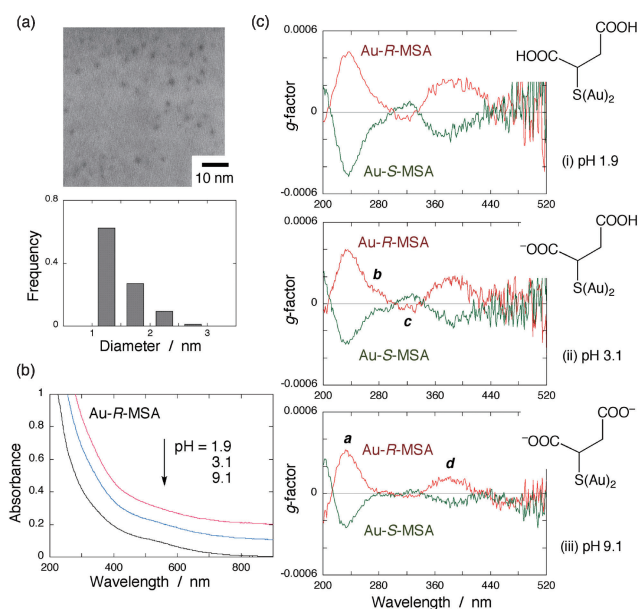


Figure 3. (a) Typical STEM image and narrow size distribution of MSA-protected Au nanoclusters. (b) Absorption spectra of Au–(*R*)-MSA recorded at different pH solutions. Spectra are offset by a constant for clarity. (c) Profiles of *g*-factor for the Au–(*R*)-MSA and Au–(*S*)-MSA nanocluster samples recorded at different pH solutions.

Figure 3b displays UV–vis absorption spectra of the Au–MSA nanocluster compounds measured at various pHs. The pH of the aqueous solution of the as-prepared nanocluster samples was 9.1, so acidification was carried out by the addition of an appropriate amount of HCl solution. In each spectrum, almost identical and monotonically increasing absorbance toward shorter wavelengths was observed. The result is in good agreement with the size of the Au nanoclusters determined by STEM (<ca. 2 nm in diameter), which scarcely supports the plasmon excitation characteristics.¹⁰ In addition, these nanoclusters were stable in a wide range of pHs, from ca. 2 to ca. 9, and absorption spectra were not influenced by protonation–deprotonation stimuli for MSA ligands.

Figure 3c shows the chiroptical responses of the (*R*)-/(*S*)-MSA-protected Au nanocluster samples at various pH values. The typical ionization forms of MSA are also shown. The spectra are shown as profiles of the anisotropy factor (*g*-factor) determined as $\Delta\epsilon/\epsilon$, where $\Delta\epsilon$ and ϵ express the intensity of the molar dichroic absorption and molar extinction coefficient, respectively. Importantly, the chiroptical activity of the chiral MSA-protected Au nanoclusters is pH-responsive. It should be further emphasized that nanoclusters protected by (*S*)-MSA show an almost complete mirror image of the chiroptical response of that protected by (*R*)-MSA. The mirror image relationship in metal-based electronic transition regions suggests that these nanoclusters have a well-defined stereostructure.¹¹ Spectral shapes were, overall, similar with each other; but with a close inspection, we found that (i) upon acidification (pH 3.1 and 1.9), two new peaks (referred to as bands *b* and *c* (Figure 3c) detected at ca. 280 and ca. 320 nm, respectively) were resolved in addition to band *a* (extremum at ca. 235 nm) and band *d* (extremum at ca. 400 nm) that are also present in the basic solution (pH 9.1); (ii) the response amplitudes for bands *a* and *d* were successively enhanced with a decrease in pH, but those for bands *b* and *c* were saturated at pH ≤ 3.1 . The

increase in the CD responses is strongly associated with that of pure MSA. On the basis of the pK_a values of MSA,⁴ two protonation–deprotonation equilibria are present in aqueous dispersion. At pH 1.9 (or 9.1), all protonated neutral (or doubly deprotonated) species are predominant.¹² At pH 3.1, the existed species are singly and doubly protonated forms of MSA. Hence, the presence of ionized carboxylate (or non-ionized carboxy) groups strongly modulates the chiroptical response (and overall dissymmetric field) of the Au nanoclusters. In consideration with the significant pH dependence of the electronic states and stable geometries of MSA deduced from the quantum chemical calculations, the observed pH-responsive behaviors would reasonably stem from *both* the electronic and conformational origins of the MSA ligands.

It is now established that the Au–S interface in small Au nanoclusters consists of staples or semi-rings of RS–(Au–SR)_n, so the thiolate-protected Au nanoclusters can be expressed in the “divide and protect” notation; for example, Au₂₅(SR)₁₈ = Au₁₃[RS–(Au–SR)₂]₁₃.¹³ Moreover, in a molecule-like cluster model, theoretical considerations have revealed that metal-based electronic transitions with higher energy (than the HOMO–LUMO transition) are imparted with ligand character.¹⁴ On this basis, it is reasonable to assign that the characteristic chiroptical signals observed at ca. 260–500 nm in the present Au nanoclusters should arise from the electronic state mixing of the MSA ligands and staple gold atoms, as has been discussed for chiral 2-phenylpropane-1-thiol-protected Au₂₅ clusters.¹⁴ Therefore, an enhancement of the chiroptical activity for the Au nanoclusters upon acidification (or protonation) can be explained by (I) a decrease in the conformational mobility of MSA ligands on the staples¹⁵ and/or (II) an effective CD stealing from the chiral ligand response (as a perturber), which directly transfers the rotatory strength to metal-based transitions involving the electronic mixing of the ligands and staple gold via dipole–dipole coupling.¹⁶

In mechanism (I), the ligands should be structurally (or conformationally) confined via some kinds of interaction, since the CD response can arise from the contributions of all present conformers.¹⁵ Hydrogen bond interactions may be a possible origin for a decrease in the conformational mobility.¹⁵ In aqueous solution, hydrogen bonds are formed between water and individual molecules of carboxylic acid, not between the carboxylic acids. However, when two or more MSA ligands are close together on short –S–Au–S– oligomer sites or staples of the surface, the proximal carboxy groups can approach each other, producing hydrogen bonds.

In mechanism (II), when a perturber itself exhibits a strong chiroptical response, the CD stealing works efficiently.¹⁶ In the present case, the chiroptical transition ($n-\pi^*$ transition of carboxy group) of MSA ligand, which corresponds to band *a*, can be the most probable perturber, since its chiroptical activity is positively associated with those of the other three metal-based bands, *b–d*, and thus chirality in bands *b–d* can be induced by this perturbation. In this context, the rotatory strength induced by the perturber can be expressed as

$$R \propto \frac{V_{ij}}{(\nu_j^2 - \nu_i^2)} \text{Im}(\boldsymbol{\mu}_i \cdot \boldsymbol{m}_j) \quad (1)$$

where suffices *i* and *j* denote a metal-based (ligands/staple-gold mixed) state and chiral perturber, respectively, $\boldsymbol{\mu}$ and \boldsymbol{m} the electric and magnetic transition moments, respectively, and ν is the

transition frequency. In addition, V_{ij} is the dipole–dipole interaction term, which couples the two electric transitions $\boldsymbol{\mu}_i$ and $\boldsymbol{\mu}_j$, and Im expresses the imaginary part of a dot product.¹⁶ According to this relationship, the following conditions are required to obtain large induced optical activity or rotatory strength; (i) ν_i is close to ν_j , (ii) V_{ij} is large, (iii) $\boldsymbol{\mu}_i$ and \boldsymbol{m}_j are aligned, or (iv) $\boldsymbol{\mu}_i$ and/or \boldsymbol{m}_j is large. On the basis of the quantum chemical calculations for MSA, the electric dipole strengths (determined as the square of the transition dipole moment) of the lowest transition for the neutral, singly, or doubly deprotonated MSA were 0.124, 0.025, or 0.041 (au; $\{8.478 \times 10^{-30}\}^2 \text{C}^2 \text{m}^2$), and the magnetic dipole strengths 0.282, 0.268, or 0.392 (au), respectively. This means that only the electric dipole moment of neutral MSA is significantly large, and thus it can remarkably contribute to an enhancement of V_{ij} via dipole–dipole coupling. Meanwhile, when the solution pH value is high, a blue shift of the perturber transition makes the frequency difference ($\nu_j - \nu_i$) large, which contributes to the reduction in the induced rotatory strength. Note that the geometrical factors of $\boldsymbol{\mu}_i$ and \boldsymbol{m}_j might be averaged out if the conformational fluctuations of the ligands (that is, perturber) are not sufficiently suppressed. In summary, enhancement in the chiroptical response of chiral MSA-protected Au nanoclusters was observed upon acidification of the dispersion, which could be interpreted in terms of both the electronic and conformational origins of the MSA ligands (that is, CD stealing and restriction of the ligand mobility).

The authors thank Ms. Risa Kakinoki (University of Hyogo) for helping in the optical resolution of *rac*-MSA.

References and Notes

- R. Jin, *Nanoscale* **2010**, *2*, 343.
- a) E. Ying, D. Li, S. Guo, S. Dong, J. Wang, *PLoS ONE* **2008**, *3*, e2222. b) H. Yao, O. Momozawa, T. Hamatani, K. Kimura, *Chem. Mater.* **2001**, *13*, 4692.
- H. Yao, H. Kojima, S. Sato, K. Kimura, *Langmuir* **2004**, *20*, 10317.
- A. Królikowska, J. Bukowska, *J. Raman Spectrosc.* **2007**, *38*, 936.
- T. Shiraiwa, M. Ohkubo, M. Kubo, H. Miyazaki, M. Takehata, H. Izawa, K. Nakagawa, H. Kurokawa, *Chem. Pharm. Bull.* **1998**, *46*, 1364.
- R. E. Benesch, R. Benesch, *J. Am. Chem. Soc.* **1955**, *77*, 5877.
- M. J. Frisch, et al., *Gaussian 09*, Gaussian, Inc., Wallingford CT, **2010**.
- a) J. Rétey, W. E. Hull, F. Snatzke, G. Snatzke, U. Wagner, *Tetrahedron* **1979**, *35*, 1845. b) J. Gawroński, J. Grajewski, *Org. Lett.* **2003**, *5*, 3301.
- a) A. Corma, P. Serna, *Science* **2006**, *313*, 332. b) Y. Zhu, Z. Wu, C. Gayathri, H. Qian, R. R. Gil, R. Jin, *J. Catal.* **2010**, *271*, 155.
- K. L. Kelly, E. Coronado, L. L. Zhao, G. C. Schatz, *J. Phys. Chem. B* **2003**, *107*, 668.
- a) H. Yao, *Curr. Nanosci.* **2008**, *4*, 92. b) H. Yao, K. Miki, N. Nishida, A. Sasaki, K. Kimura, *J. Am. Chem. Soc.* **2005**, *127*, 15536.
- In ref 4, SERS experiments suggested that one of the carboxylic groups of MSA (close to S atom) attached on bulk gold was partly dissociated even in pH 1.2 due to some interactions with the gold surface. It may be possible, but bear in mind that ligand structures on the clusters can be different from those on the bulk gold.
- H. Häkkinen, *Nat. Chem.* **2012**, *4*, 443.
- a) M. Zhu, H. Qian, X. Meng, S. Jin, Z. Wu, R. Jin, *Nano Lett.* **2011**, *11*, 3963. b) C. Noguez, A. Sánchez-Castillo, F. Hidalgo, *J. Phys. Chem. Lett.* **2011**, *2*, 1038.
- a) I. Frič, M. Flegel, M. Zaoral, M. Kodíček, *Eur. J. Biochem.* **1975**, *56*, 493. b) J.-G. Dong, J. Guo, I. Akritopoulou-Zanze, A. Kawamura, K. Nakanishi, N. Berova, *Chirality* **1999**, *11*, 707.
- N. Kobayashi, R. Higashi, B. C. Titeca, F. Lamote, A. Ceulemans, *J. Am. Chem. Soc.* **1999**, *121*, 12018.